Simulation of the effect of grain-boundaries in backside-passivated CIGS solar cells

Simulation of the effect of grain-boundaries in backside-passivated CIGS solar cells

Giovanna Sozzi
Department of Engineering and Architecture
University of Parma
Parma, ITALY
giovanna.sozzi@unipr.it

Roberto Menozzi
Department of Engineering and Architecture
University of Parma
Parma, ITALY
roberto.menozzi@unipr.it

***Abstract*—We carry out numerical 3D simulations of CIGS cells with back-side Al_2O_3 passivation and point contact openings in the presence of grain boundaries in the absorber. We consider CIGS cells with different absorber thickness, from 0.35 to 3 μm. For thinner absorbers (1 μm or less) we observe that GBs terminating on the Al_2O_3 are completely or almost completely passivated, while the effectiveness of the passivation decreases for thicker absorbers. GBs terminating on the point contact, instead, significantly lower the efficiency, regardless of absorber thickness. The presence of grain boundaries and the dimension of grains should therefore be taken into consideration when optimizing the back-side point contact array geometry.**

***Keywords*—Al_2O_3, CIGS, grain-boundary, rear passivation, point contact.**

I. INTRODUCTION

Cu(In, Ga)Se_2 chalcopyrite solar cells with the highest efficiency typically feature absorber layer thickness between 2 and 3 μm to ensure sufficient absorption of long wavelength light. On the other hand, in order to reduce material consumption and production cost, further thinning of CIGS absorber is desirable [1]. Unfortunately, thin and ultra-thin absorber cells suffer more from optical losses and increased recombination at the rear contact, the latter due to the proximity of the contact with the region of largest optical generation.

As observed by different groups both experimentally [2][3] and with numerical studies [4][5], surface passivation of the back surface, for example with Al_2O_3 [6], is an efficient way to mitigate the open circuit voltage loss due to recombination at the rear contact.

Although several studies have been carried out to investigate the optimal geometry of the point-contact openings in the passivation both on the front and the rear side of CIGS cells [7][8], previous works have not dealt with the possible influence of grain boundaries (GBs) on the performance of rear-passivated solar cells. Since optimized back-side point contact geometries are in the range of hundreds of nanometers [5], interaction with grain boundaries is likely, and numerical investigation can help understand its impact.

The geometrical optimization of cells with back-side passivation and point contacts by means of three-dimensional (3D) simulations has been treated in a previous work [5]: starting from those results, which were obtained without considering GBs, we focus here on the effect of grain boundaries on the performance of passivated cells with different CIGS thickness. Results provided by modelling can contribute to gain further insight of the role of GBs in rear-passivated solar cells, and lead to better understanding of experimental data, and optimized cell design.

II. MODELED CELL

Using the Synopsys Sentaurus-Tcad suite, we simulated the solar cells sketched in Fig. 1: they feature absorbers of different thickness (namely, t_{CIGS} = 3, 2, 1, 0.5 and 0.35 μm), with a 600 nm $MoSe_2$/Mo contact layer placed under the 10-nm back-side Al_2O_3 passivation. A 105 nm-thick MgF_2 anti-reflecting coating is included.

Since proper description of the cell geometry with openings in the rear passivation requires a 3D approach, we simulate cylindrical cells with 1 μm-radius – corresponding to half the point contact pitch – with the symmetry axis passing through the center of the point contact (right sidewalls of the structures in Fig. 1); the point contact radius is wpc/2 (Fig. 1). The GB is positioned 500 nm away from the center of the contact (GB_pos

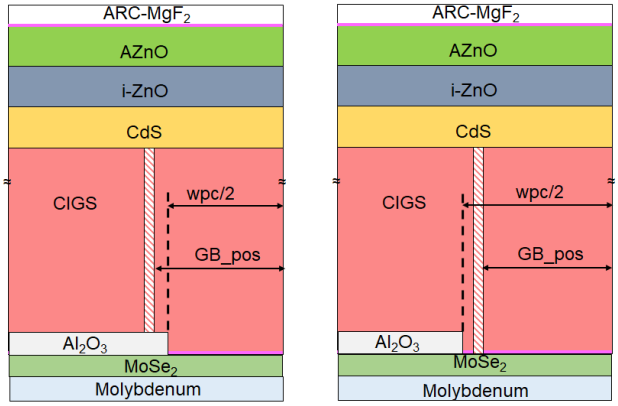

Fig. 1. Schematic cross-section of the simulated cells. The red-hatched region indicates the GB. The simulated structures are 3D cylindrical cells where the axis of the cylinder is the right sidewall.

= 500 nm, Fig. 1): this means that our 3D simulations feature a central cylindrical grain with 500 radius surrounded by a GB.

We considered two scenarios: a GB terminating on the passivation (wpc/2 = 490 nm, Fig. 1a), and one terminating on the point contact (wpc/2 = 510 nm, Fig. 1b). The small difference (20 nm) of point contact radius between the two cases does not in itself appreciably affect the cell performance [5]. As a reference, we also carried out simulations of all the cells with point contacts and no GB.

The cell is illuminated by the standard AM1.5G solar spectrum, and the light propagation through the cell is calculated by the TMM (Transfer Matrix Method) approach. The main cell parameters are reported in Table I and in [9].

TABLE I. MATERIAL PARAMETERS USED IN THE SIMULATIONS

Material	AZnO	i-ZnO	CdS	CIGS
Eg (eV)	3.3	3.3	2.4	1.2
Thickness (nm)	200	80	30	var
$N_{D/A}$ (cm^{-3})	$4\cdot10^{19}$ (D)	10^{17} (D)	10^{17} (D)	10^{16} (A)
ΔEc (eV)	-	-0.2		0.3
Bulk Trap				
Density (cm^{-3})	10^{16}		$3\cdot10^{15}$	$6.67\cdot10^{14}$
Energy (eV)	midgap			
Capture cross section (cm^2)	$\sigma_e: 10^{-15}$ $\sigma_h: 10^{-12}$		$\sigma_e: 10^{-15}$ $\sigma_h: 10^{-12}$	$\sigma_e: 10^{-15}$ $\sigma_h: 10^{-15}$

The GB is modeled as a thin (2 nm) region decorated by donor traps; donor defects have been found to be more detrimental for the cell performance than acceptor defects [10]. The defects have density $N_{TGB} = 5\cdot10^{18}$ cm^{-3}, and are located at $E_{TGB} = 0.35$ eV below the conduction band; their capture cross-section (for both electrons and holes) is 10^{-18} cm^2 [11][12].

Fig. 2 shows the conduction band and SRH recombination profiles under short circuit condition along a horizontal line 1 µm below the CdS/CIGS interface for the 2 µm-absorber cell with (solid lines) and without (dashed lines) GB. The presence of donor-like traps within the GB determines the downward band-bending (black solid line) and causes electrons to accumulate along the GB [11] [13] . As a result, in the region around the GB the SRH recombination increases (red solid line) with respect to the case with no GB (red dashed line).

At the interface between CIGS and the Al_2O_3 passivating layer, the recombination velocity is set at $v_P = 10^4$ cm/s, corresponding to a case of partial chemical passivation, while at the back contact the recombination velocity is $v_R = 10^6$ cm/s. Finally, field-effect passivation is not accounted for in the simulations, that is no charge is included in the passivating material [6][14].

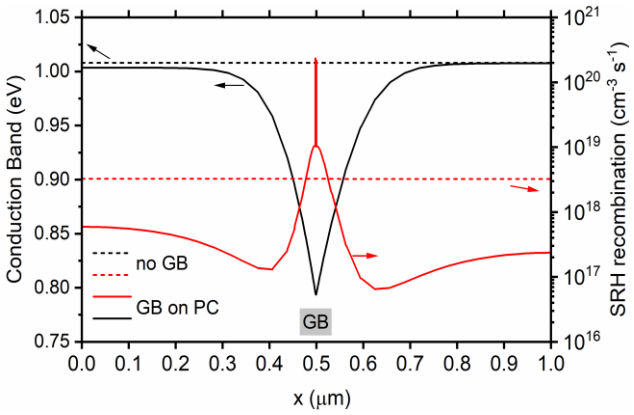

Fig. 2. Conduction band (black lines) and SRH recombination profiles (red lines) along a horizontal line 1 µm below the CdS/CIGS interface, at short-circuit condition. Solid and dashed lines refer to the cell with GB and without GB, respectively. The absorber thickness is 2 µm; GB at x = 0.5 µm.

III. RESULTS AND DISCUSSION

Figs. 3 and 4 show the performance parameters of cells with different absorber thickness ranging from 3 µm down to 0.35 µm, for the cases of no GB, GB terminating on the backside passivation (as in Fig. 1a), and GB terminating on the point contact (as in Fig. 1b). These are the main observations stemming from Figs. 3 and 4.

(1) V_{OC} (Fig. 3, top) is significantly reduced by the presence of the GB, due to increased recombination. A GB terminating

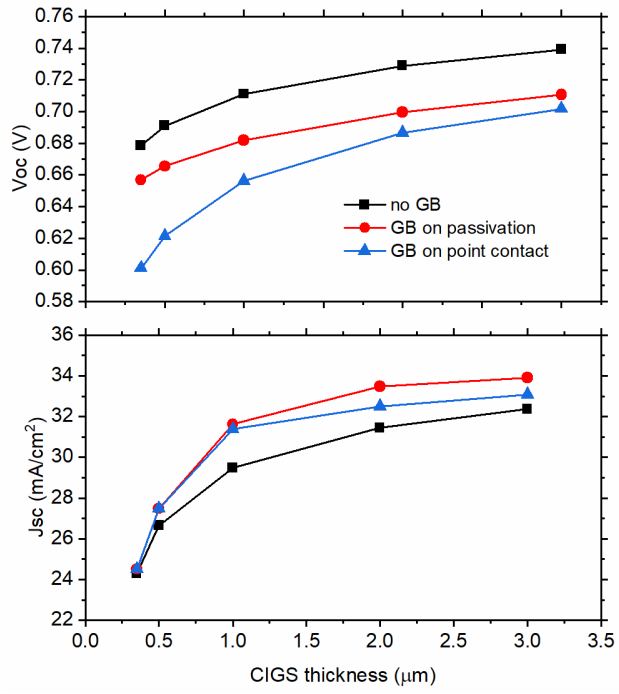

Fig. 3. Voc and Jsc versus CIGS absorber thickness in the cases of absence of GB (black line and squares), GB ending on passivation (red line and circles), and GB terminating on point contact (blue line and triangles).

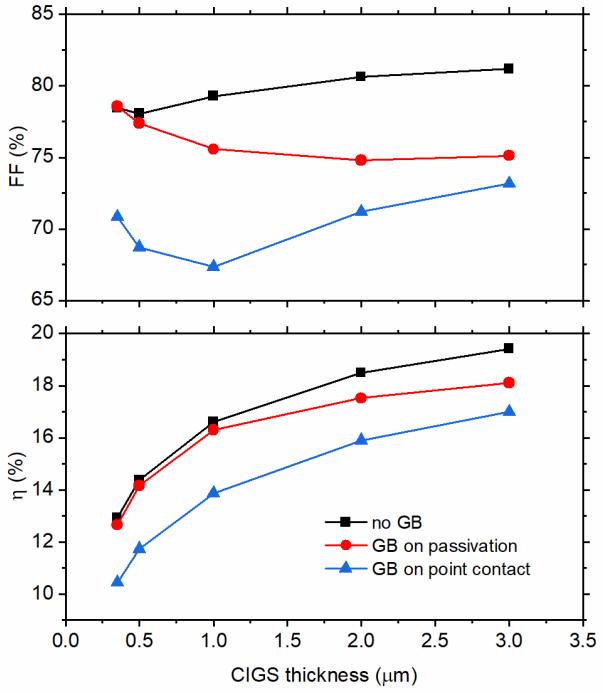

Fig. 4. FF and η versus the CIGS absorber thickness in the cases of absence of GB (black line and squares), GB ending on passivation (red line and circles), and GB terminating on point contact (blue line and triangles).

on the passivation is less harmful than one terminating on the point contact, i.e., the backside Al_2O_3 layer is effective also for GB passivation. As can be expected, the beneficial effect of the passivation of the GB tends to be smaller for thick absorbers, where the detrimental effect of the whole length of the GB dominates over the effect of the back-contact.

The effect of GB on SRH recombination is shown in Fig. 2 for the 2 μm-absorber cell. As an example, in the 2 μm-absorber cell at a voltage bias of 0.67 V, corresponding to the Voc of the cell with GB terminating on the point contact, the SRH recombination integrated over the CIGS volume is

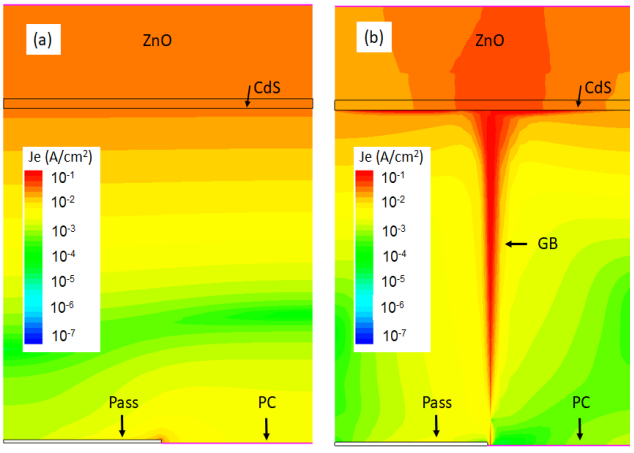

Fig. 5. Electron current density maps at short-circuit condition for the cell with absorber thickness of 1 μm; (a) no GB; (b) GB ending on point-contact.

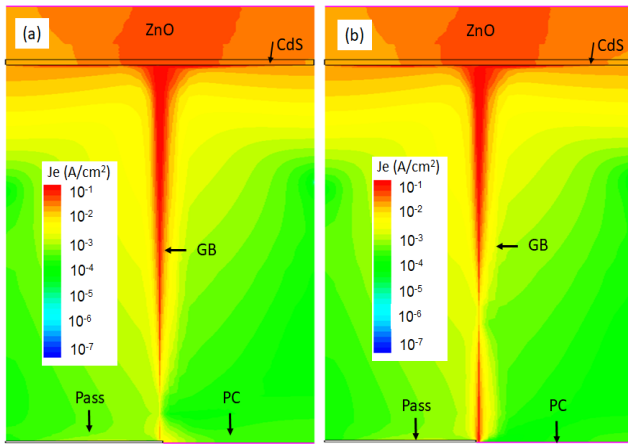

Fig. 6. Electron current density maps at short-circuit condition for the cell with absorber thickness of 2 μm; (a) GB ending on the passivation; (b) GB ending on the point-contact.

$4.67 \cdot 10^9\ s^{-1}$, to be compared with $2.66 \cdot 10^9\ s^{-1}$ in the corresponding cell with no GB.

(2) J_{SC} (Fig. 3, bottom) is somewhat larger in the presence of the GB, for absorbers thicker than 0.5 μm. This is due to the downward-bent bands at the GB helping channel the electron current to the cathode, as shown by Fig. 5. Not surprisingly, this effect is more significant in thicker absorbers.

However, when the GB terminates on the point contact, some channeling of the electron current towards the anode takes place as well (see Fig. 6b), which results in a small reduction of J_{SC} with respect to the case of GB terminating on the passivation.

Quantitatively, at short circuit the electron current density at the anode (reducing J_{SC}) is about 0.25 mA/cm^2 in Fig. 6a, and 1.35 mA/cm^2 in Fig. 6b, while the hole current exiting the anode is practically the same; as a consequence, the beneficial effect of the passivation is reduced when the GB ends on the point contact (compare the red and blue lines in Fig. 3, bottom).

(3) The FF (Fig. 4, top) is significantly affected by the presence of a GB terminating on the point contact, regardless of the absorber thickness.

When the GB terminates on the passivation, instead, the FF hardly suffers for absorbers up to 0.5 μm thick, but is degraded more and more as the thickness increases, due to the dominating effect of the GB length.

Fig. 7 shows the total current and the electron current component at the anode contact versus bias voltage in the dark for cells with GB terminating on passivation (black lines) and on the point contact (red lines) in the case of 1 μm-absorber, corresponding to a FF difference of 8.2% absolute between the two structures (see Fig. 4). With the GB ending on the point contact, a larger dark current (red solid line), mainly due to electrons (red dot-dash line) flowing along the GB, adds to the photo-generated current causing the observed large degradation of FF.

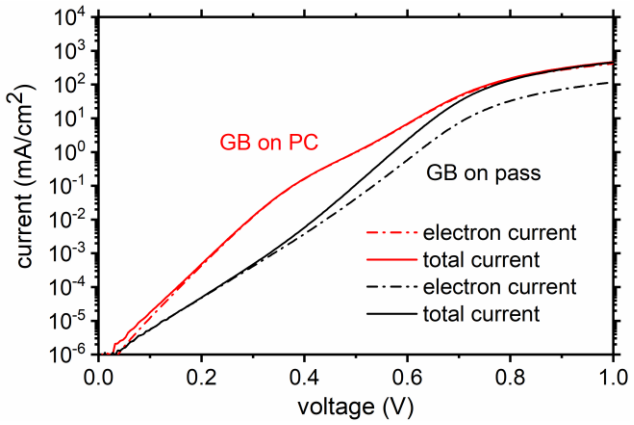

Fig. 7. Total current density (solid lines) and electron current density (dashed-dotted lines) in the dark at the anode for the cell with absorber thickness of 1 μm; red curves: GB ending on point-contact black curves: GB ending on passivation.

(4) As a consequence of (1)-(3), the efficiency (Fig. 4, bottom), which is significantly degraded by the presence of a GB terminating on the point contact ($|\Delta\eta| > 2\%$ absolute, regardless of the absorber thickness), is partially (for thicker absorbers) or totally (for thinner absorbers) restored in the case where the GB terminates on the passivation.

IV. Conclusions

We carried out numerical 3D simulations to evaluate the effect of back-side Al_2O_3 passivation with point contact openings in connection with the presence of grain boundaries (GBs) in the absorber of CIGS cells with different absorber thickness.

We showed that the position of the GB with respect to the point contact has significant impact on the cell's performance and on the effectiveness of the back-side passivation.

For thinner absorbers (1 μm or less), the cells with GBs terminating on the passivation show practically the same efficiency as those without GBs, while the benefit of the passivation decreases for 2 μm and 3 μm absorbers.

On the other hand, when the GB terminates on the point contact, the efficiency is consistently lower by more than 2% absolute than in the corresponding GB-free case, regardless of absorber thickness.

This indicates that the presence of grain boundaries and the dimension of grains do influence the effectiveness of back-side passivation, and should therefore be taken into consideration in the optimization of the point contact array geometry.

V. References

[1] N. Naghavi et al., "Ultrathin Cu(In,Ga)Se2 based solar cells," Thin Solid Films, vol. 633, pp. 55–60, 2017. https://doi.org/10.1016/j.tsf.2016.11.029.

[2] B. Vermang, V. Fjallström, X. Gao, and M. Edoff, "Improved rear surface passivation of Cu(In,Ga)Se2 solar cells: A combination of an Al2O3 rear surface passivation layer and nanosized local rear point contacts," IEEE J. Photovoltaics, vol. 4, no. 1, pp. 486–492, 2014. https://doi.org/10.1109/JPHOTOV.2013.2287769.

[3] S. Choi, Y. Kamikawa, J. Nishinaga, A. Yamada, H. Shibata, and S. Niki, "Lithographic fabrication of point contact with Al2O3 rear-surface-passivated and ultra-thin Cu(In,Ga)Se2 solar cells," Thin Solid Films, vol. 665, no. January, pp. 91–95, 2018. https://doi.org/10.1016/j.tsf.2018.08.044.

[4] R. Kotipalli et al., "Addressing the impact of rear surface passivation mechanisms on ultra-thin Cu(In,Ga)Se 2 solar cell performances using SCAPS 1-D model," Sol. Energy, vol. 157, pp. 603–613, 2017. https://doi.org/10.1016/j.solener.2017.08.055.

[5] G. Sozzi, S. Di Napoli, M. Carrisi, and R. Menozzi, "Assessing the impact of rear point-contact/passivation on CIGS cells with different absorber thickness and grading," in: Proc. 2018 IEEE 7th World Conf. Photovolt. Energy Conversion, WCPEC 2018 - A Jt. Conf. 45th IEEE PVSC, 28th PVSEC 34th EU PVSEC, pp. 3044–3047, 2018. https://doi.org/10.1109/PVSC.2018.8548312.

[6] W.-W. Hsu et al., "Surface passivation of Cu(In,Ga)Se2 using atomic layer deposited Al2O3," Appl. Phys. Lett., vol. 100, no. 2, p. 023508, 2012. https://doi.org/10.1063/1.3675849.

[7] G. Sozzi et al., "Designing CIGS solar cells with front-side point contacts," in: Proc 2015 IEEE 42nd Photovoltaic Specialist Conference (PVSC), pp. 1–5, 2015. https://doi.org/10.1109/PVSC.2015.7355691

[8] A. Bercegol, B. Chacko, R. Klenk, I. Lauermann, M. C. Lux-Steiner, and M. Liero, "Point contacts aBercegol, A., Chacko, B., Klenk, R., Lauermann, I., Lux-Steiner, M. C., & Liero, M. (2016). Point contacts at the copper-indium-gallium-selenide interface - A theoretical outlook. Journal of Applied Physics, 119(15). https://doi.org/10.106," J. Appl. Phys., vol. 119, no. 15, 2016. https://doi.org/10.1063/1.4947267.

[9] G. Sozzi et al., "Analysis of Ga grading in CIGS absorbers with different Cu content," in: Proc. IEEE 43rd Photovoltaic Specialists Conference (PVSC), p.2279-2282, 2016. https://doi.org/10.1109/PVSC.2016.7750042.

[10] N. Nicoara et al., "Direct evidence for grain boundary passivation in Cu(In,Ga)Se2 solar cells through alkali-fluoride post-deposition treatments," Nat. Commun., vol. 10, pp. 1–8, 2019. https://doi.org/10.1038/s41467-019-11996-y.

[11] M. Gloeckler, J. R. Sites, and W. K. Metzger, "Grain-boundary recombination in Cu (In,Ga) Se2 solar cells," J. Appl. Phys., vol. 98, no. 11, 2005. https://doi.org/10.1063/1.2133906.

[12] K. Taretto, U. Rau, K. Taretto, and U. Rau, "Numerical simulation of carrier collection and recombination at grain boundaries in Cu (In , Ga) Se2 solar cells," J. Appl. Phys., vol. 094523, no. May 2013, 2008. https://doi.org/10.1063/1.2917293.

[13] R. Baier, C. Leendertz, D. Abou-Ras, M. C. Lux-Steiner, and S. Sadewasser, "Properties of electronic potential barriers at grain boundaries in Cu(In,Ga)Se2thin films," Sol. Energy Mater. Sol. Cells, vol. 130, pp. 124–131, 2014. https://doi.org/10.1016/j.solmat.2014.07.002.

[14] R. Kotipalli, B. Vermang, J. Joel, R. Rajkumar, M. Edoff, and D. Flandre, "Investigating the electronic properties of Al2O3/Cu(In,Ga)Se2 interface," AIP Adv., vol. 5, no. 10, 2015. https://doi.org/10.1063/1.4932512.